Advances in Science, Technology & Innovation
IEREK Interdisciplinary Series for Sustainable Development

Simon Elias Bibri · Anna Visvizi ·
Orlando Troisi *Editors*

Advancing Smart Cities

Sustainable Practices, Digital Transformation, and IoT Innovations

IEREK
RESEARCH & KNOWLEDGE ENRICHMENT

Springer

Advances in Science, Technology & Innovation

IEREK Interdisciplinary Series for Sustainable Development

Editorial Board

Anna Laura Pisello, Department of Engineering, University of Perugia, Italy

Dean Hawkes, University of Cambridge, Cambridge, UK

Hocine Bougdah, University for the Creative Arts, Farnham, UK

Federica Rosso, Sapienza University of Rome, Rome, Italy

Hassan Abdalla, University of East London, London, UK

Sofia-Natalia Boemi, Aristotle University of Thessaloniki, Greece

Nabil Mohareb, Faculty of Architecture—Design and Built Environment, Beirut Arab University, Beirut, Lebanon

Saleh Mesbah Elkaffas, Arab Academy for Science, Technology and Maritime Transport, Cairo, Egypt

Emmanuel Bozonnet, University of La Rochelle, La Rochelle, France

Gloria Pignatta, University of Perugia, Italy

Yasser Mahgoub, Qatar University, Qatar

Luciano De Bonis, University of Molise, Italy

Stella Kostopoulou, Regional and Tourism Development, University of Thessaloniki, Thessaloniki, Greece

Biswajeet Pradhan, Faculty of Engineering and IT, University of Technology Sydney, Sydney, Australia

Md. Abdul Mannan, Universiti Malaysia Sarawak, Malaysia

Chaham Alalouch, Sultan Qaboos University, Muscat, Oman

Iman O. Gawad, Helwan University, Helwan, Egypt

Anand Nayyar, Graduate School, Duy Tan University, Da Nang, Vietnam

Series Editor

Mourad Amer, International Experts for Research Enrichment and Knowledge Exchange (IEREK), Cairo, Egypt

Advances in Science, Technology & Innovation (ASTI) is a series of peer-reviewed books based on important emerging research that redefines the current disciplinary boundaries in science, technology and innovation (STI) in order to develop integrated concepts for sustainable development. It not only discusses the progress made towards securing more resources, allocating smarter solutions, and rebalancing the relationship between nature and people, but also provides in-depth insights from comprehensive research that addresses the **17 sustainable development goals (SDGs)** as set out by the UN for 2030.

The series draws on the best research papers from various IEREK and other international conferences to promote the creation and development of viable solutions for a **sustainable future and a positive societal** transformation with the help of integrated and innovative science-based approaches. Including interdisciplinary contributions, it presents innovative approaches and highlights how they can best support both economic and sustainable development, through better use of data, more effective institutions, and global, local and individual action, for the welfare of all societies.

The series particularly features conceptual and empirical contributions from various interrelated fields of science, technology and innovation, with an emphasis on digital transformation, that focus on providing practical solutions to **ensure food, water and energy security to achieve the SDGs.** It also presents new case studies offering concrete examples of how to resolve sustainable urbanization and environmental issues in different regions of the world.

The series is intended for professionals in research and teaching, consultancies and industry, and government and international organizations. Published in collaboration with IEREK, the Springer ASTI series will acquaint readers with essential new studies in STI for sustainable development.

ASTI series has now been accepted for Scopus (September 2020). All content published in this series will start appearing on the Scopus site in early 2021.

Simon Elias Bibri • Anna Visvizi •
Orlando Troisi
Editors

Advancing Smart Cities

Sustainable Practices, Digital Transformation, and IoT Innovations

A culmination of selected research papers from the International Conference on Future Smart Cities (FSC-5th), With Xiamen University, Malaysia

Springer

Editors
Simon Elias Bibri
Institute of Computer and Communication Sciences (IINFCOM)
School of Architecture, Civil and Environmental Engineering (ENAC)
Media and Design Laboratory (LDM)
Swiss Federal Institute of Technology Lausanne (EPFL)
Lausanne, Switzerland

Anna Visvizi
SGH Warsaw School of Economics
Effat University
Jeddah, Saudi Arabia

Orlando Troisi
Department of Political and Communication Sciences
University of Salerno
Fisciano, Italy

ISSN 2522-8714 ISSN 2522-8722 (electronic)
Advances in Science, Technology & Innovation
IEREK Interdisciplinary Series for Sustainable Development
ISBN 978-3-031-52302-1 ISBN 978-3-031-52303-8 (eBook)
https://doi.org/10.1007/978-3-031-52303-8

© The Editor(s) (if applicable) and The Author(s), under exclusive license to Springer Nature Switzerland AG 2024

This work is subject to copyright. All rights are solely and exclusively licensed by the Publisher, whether the whole or part of the material is concerned, specifically the rights of translation, reprinting, reuse of illustrations, recitation, broadcasting, reproduction on microfilms or in any other physical way, and transmission or information storage and retrieval, electronic adaptation, computer software, or by similar or dissimilar methodology now known or hereafter developed.
The use of general descriptive names, registered names, trademarks, service marks, etc. in this publication does not imply, even in the absence of a specific statement, that such names are exempt from the relevant protective laws and regulations and therefore free for general use.
The publisher, the authors, and the editors are safe to assume that the advice and information in this book are believed to be true and accurate at the date of publication. Neither the publisher nor the authors or the editors give a warranty, expressed or implied, with respect to the material contained herein or for any errors or omissions that may have been made. The publisher remains neutral with regard to jurisdictional claims in published maps and institutional affiliations.

This Springer imprint is published by the registered company Springer Nature Switzerland AG
The registered company address is: Gewerbestrasse 11, 6330 Cham, Switzerland

Paper in this product is recyclable.

Scientific Committee

Gabriel Gomes de Oliveira, University of Campinas, São Paulo, Campinas, Brazil
Rita Yi Man Li, Center Hong Kong Shue Yan University, China
Hossein Hossein Alakbeikl, DISA-MIS Department, University of Salerno, Italy
Giovanni Baldi, University of Salerno, Italy
Gianluca Guazzo, University of Salerno, Italy
Samaa Radi Badawi, University of Mansoura, Egypt
Partson Paradza, BA ISAGO University, Bostawana
Krzysztof Karwowski, SGH Warsaw School of Economics, Poland
Ernestyna Szpakowska-Loranc, Cracow University, Poland
Samah El Khateeb, Ain Shams University, Egypt
Senthil Kumar Jagatheesaperumal, Mepco Schlenk Engineering College, India
Marco Seccaroni, Università degli Studi di Perugia, Italy
Alshimaa Aboelmakarem Farag, Zagazig University, Egypt
Abdulaziz I. Almulim, College of Architecture and Planning, Imam Abdulrahman Bin Faisal University, Dammam, Saudi Arabia
Parisa Sabbagh, University of Palermo, Italy
Vilma Çekani, University of Salerno, Italy
Rahma M. Doheim, Al Yamamah University, Saudi Arabia
Yuanping Yu, SGH Warsaw School of Economics, Poland
Gennaro Maione, University of Salerno, Italy
Sivaparthipan CB, Tagore Institute of Engineering and Technology, India

The Editors warmly thank all the Reviewers who have contributed their authority to the double-blind review process, to ensure the quality of this publication.

Preface

The FSC (Future Smart Cities) conference series has established itself as a highly influential and dynamic platform that explores the confluence of advanced Information and Communication Technologies (ICT) and emerging models for sustainable urban development. The conference serves as a vital catalyst in illuminating the diverse applications of manufacturing robotics, big data, the internet of things, and artificial intelligence, all aimed at enhancing the core of the urban environment. Consequently, it consistently draws the attention of policymakers, researchers, and business leaders, who collectively contribute their extensive expertise towards shaping a vision of the future.

The volume presents a compilation of research papers that vividly illustrate the transformative power of computational and data-driven technologies on the global landscape. The goal for urban functionality is to foster economic growth and streamline government services, ultimately enhancing the quality of life for citizens through the integration of intelligent technologies.

Authored by pioneers in the field, these high-quality research papers are an integral part of the forthcoming 5th edition of the FSC (Future Smart Cities) conference. The primary objective of this conference is to showcase the global significance of smart cities. It offers a unique opportunity for participants to exchange innovative ideas and engage with the leading experts and innovators in the field.

In light of the remarkable developments taking place in urban environments worldwide, the theme of this 5th edition of the FSC revolves around “Reshaping Cities for a Sustainable Future.” This theme encapsulates the pressing need to explore innovative ways to ensure that our urban spaces are not only smart but also sustainable. It acknowledges the growing challenges associated with rapid urbanization, ecological degradation, climate change, and resource constraints. By aligning technology with the principles of sustainability, the conference seeks to inspire pioneering strategies that will guide the future development of our cities.

The proceedings contribute to the advancement of various domains, including intelligible building design, smart buildings and grids, inclusive resilience, green urbanism, and city information models. These exceptional ideas, and many more, are specifically tailored to resonate with policymakers, researchers, and business leaders who are eager to drive transformative change within the urban landscape, thereby shaping the narrative of cities for future generations.

Lausanne, Switzerland

Simon Elias Bibri
Senior Research Scientist and Blue City
Project Coordinator

Acknowledgments

We extend our sincere gratitude to the three editors and the diligent editorial team at IEREK for their unwavering support and expertise in bringing this publication to fruition and their commitment to fostering knowledge exchange in the field of sustainable urban development. We would also like to express our sincere appreciation to the dedicated reviewers who invested their time and effort in evaluating the submitted papers. Their insightful feedback played a pivotal role in maintaining the high quality and academic rigor of this volume. Our heartfelt thanks go out also to the authors who contributed their outstanding research papers, sharing their innovative ideas and insights into the future of smart and sustainable cities. Their collective expertise is the cornerstone of this publication. Lastly, but by no means least, we acknowledge the continued support of IEREK in advancing the global dialogue on smart cities. This collaborative endeavor would not have been possible without their visionary approach to disseminating knowledge. Thank you to all who have contributed to this volume and to the ongoing discourse surrounding sustainable urban development.

Introduction

In the contemporary era of rapid urbanization and technological advancement, the world is undergoing an unprecedented urban transformation. As our global population continues to grow, cities are rapidly expanding to accommodate the influx of people and bolstering their strategies to address the multifaceted challenges of environmental, economic, and social sustainability. According to the United Nations, over half of the world's population currently resides in urban areas, and this number is projected to rise to 68% by 2050. Smart cities as the epicenters of human innovation and progress have emerged in response to the growing urbanization and the enormous challenges of sustainability. These urban environments are evolving, adapting, and reinventing themselves, integrating technology and sustainability in novel ways. The book *Advancing Smart Cities—Sustainable Practices, Digital Transformation, and IoT Innovations*, is an exploration of this major shift, a journey through the intricate and multifaceted world of smart cities.

A smart city is a concept that represents the intersection of urban development, technological innovation, and sustainability. It envisions a future where cities harness the power of technology to enhance the quality of life for their citizens, ensure efficient resource management, and reduce environmental impact. The core idea is to make urban living more accessible, efficient, and enjoyable, and in doing so, to build a more sustainable future. Smart cities seek to address a wide array of urban challenges, from traffic congestion and pollution to energy consumption and public safety, by leveraging cutting-edge technologies and data-driven insights. The very essence of smart cities lies in their ability to connect the physical world with the digital realm, transforming urban environments into responsive and adaptive entities.

The driving force behind the smart city movement is the convergence of digital transformation, the proliferation of the Internet of Things (IoT), and the power of Artificial Intelligence (AI) The digital revolution has unleashed a wave of innovation that is transforming how cities are planned, managed, governed, and experienced. From intelligent transportation systems and energy-efficient buildings to data-driven healthcare and responsive governance, smart cities are becoming the proving grounds for digital innovation. IoT and AI, on the other hand, represents the interconnectedness and intelligence of everyday objects through the internet and machine learning and deep learning models, enabling them to communicate, collect data, and make decisions autonomously. This technology is the lifeblood of smart cities, enabling the seamless flow of information and automation that underpins their operations.

"Advancing Smart Cities" particularly explores the dynamic intersection of digital transformation and IoT innovation, providing an in-depth exploration of the strategies, technologies, and best practices that are propelling smart cities forward. Through the pages of this book, readers will embark on a journey to discover the intricate ways in which cities worldwide are using technology to enhance urban living, foster economic growth, and safeguard the environment.

This book is designed to be an essential resource for urban planners, policymakers, technologists, researchers, and anyone intrigued by the future of cities. We aim to provide a comprehensive overview of the various aspects of smart cities, from their roots to the latest cutting-edge solutions. Our contributors, experts in their respective fields, have shared their knowledge and insights to offer a broad and insightful perspective on the transformation of cities into intelligent, responsive ecosystems.

The book is divided into four parts, each addressing critical aspects of smart cities.

Sustainable Smart Cities and Green Buildings

In the first part: *Sustainable Smart Cities and Green Buildings*, the book delves into the core principles of sustainability within the context of smart city development. It explores the vital role of green building practices in creating eco-friendly urban environments. Readers will gain insight into the use of sustainable materials, energy-efficient designs, and innovative architectural approaches that contribute to reducing the environmental footprint of smart cities. This part also discusses the broader concept of sustainable urban planning and the importance of integrating environmental considerations into every facet of city development.

Digital Transformation and Interaction Strategies

In the second part: *Digital Transformation and Interaction Strategies* delves into the heart of the digital revolution in smart cities. It offers an in-depth exploration of how digital transformation is reshaping urban landscapes, enhancing the quality of life, and optimizing city operations. Readers will discover strategies for creating seamless interactions between city systems, residents, and various stakeholders. This part highlights the importance of user-friendly interfaces, data-driven decision-making, and the empowerment of citizens through digital platforms. It underscores the significance of real-time feedback and the dynamic exchange of information as pivotal elements in building smarter, more connected cities.

Internet of Things, Big Data Analysis and Cloud Computing

In the third part: *Internet of Things, Big Data Analysis and Cloud Computing*, the book explores the fundamental technologies underpinning smart cities. It delves into the Internet of Things (IoT) and its role in connecting urban infrastructure, collecting data, and enabling automation. This part also emphasizes the crucial role of big data analysis and cloud computing in processing and making sense of the vast amounts of data generated in smart cities. Readers will gain an understanding of how these technologies work together to provide valuable insights, optimize resource management, and enhance city services.

Smart Living: Healthcare, Education, Transportation and Agriculture

The final part: *Smart Living: Healthcare, Education, Transportation, and Agriculture*, shifts focus to the practical application of smart city technologies in various aspects of daily life. It delves into how these innovations impact healthcare, education, transportation, and agriculture. Readers will explore how IoT devices are revolutionizing healthcare delivery, how educational systems are adapting to digital learning, and how smart transportation systems are reducing congestion and improving mobility. This section also discusses the role of technology in advancing precision agriculture and enhancing food security in urban settings, underscoring the holistic transformation of urban living through smart solutions.

These expanded descriptions provide a more comprehensive view of each section. In each part, we present case studies, real-world examples, and expert analyses to provide useful insights into the subject matter. By the end of the book, readers will have a deep understanding of the complexity and potential of smart cities, as well as the challenges that must be addressed to fulfill their promise.

As we navigate through the pages of "Advancing Smart Cities: Sustainable Practices, Digital Transformation, and IoT Innovations," we hope that you will be inspired by the possibilities that smart cities offer and recognize the pivotal role that technology plays in reshaping our urban future. The world is changing, and cities are at the forefront of this transformation. With the guidance of this book, we invite you to embark on a journey of discovery and exploration, unearthing the innovations that are shaping the cities of tomorrow.

Lausanne, Switzerland Simon Elias Bibri
October 2023

Contents

Sustainable Smart Cities and Green Buildings

Digital Transformation and Interaction Strategies

Internet of Things, Big Data Analysis and Cloud Computing

Smart Living: Healthcare, Education, Transportation and Agriculture

Sustainable Smart Cities and Green Buildings

Design and Characterization of Compact On-Metal UHF RFID Tag Antenna for Smart Cities

Jiazheng Zhao, Chia Chao Kang, Jian Ding Tan, M. M. Ariannejad, and Steven Yoong Choong Hoong

Abstract

In today's smart cities, the use of passive Radio-frequency Identification (RFID) tags gained popularity in access control, file tracking for healthcare, supply chain management in logistics, smart labels, vehicle tracking identification and others. The main advantages of using passive RFID tags are low cost and not requiring an internal power source to activate the tag. However, the metal surface has always been a challenge to passive RFID tags due to metal interference. The interference was caused by reflected energy from metal surfaces that were emitted from the RFID readers. As a result, the tag was unable to both transmit and receive information. This is also inconvenient to users as metal must not be present in the surroundings where the RFID tag is installed. As such, this paper proposed a compact passive Ultra High Frequency (UHF) RFID tag that can be installed on metal surfaces. To meet compactness requirements and flexibility over impedance matching, the antenna is designed in S-shaped by using computer simulation technology CST software. Two methods are used to model the antenna tag which firstly is to increase the gap between the antenna and the metal surface, secondly to place absorbing material between the antenna and metal surface. PP-4 flexible foam is used as the gap and three polyimide films are inserted which act as absorbing materials to ensure that the tag functions well in harsh environments for smart city sustainability. Thus, as a result, based on the Friis transmission equation, the antenna tag can achieve a read distance of up to 4.815 m.

Keywords

Compact • On-metal • RFID • S-shaped

1 Introduction

Nowadays, numerous industries have undergone significant changes as a result of technological progress in the realms of information and communication technologies, digitalization and networking (Kang et al., 2023). RFID employs wireless technology to utilize radio frequencies (RF) for the purpose of interacting with distinctively recognizable devices referred to as tags (Fahmy et al., 2019). RFID supports a wide range of IoT applications due to its high throughput, non-contact readability, tag functionality and most importantly low cost (Munoz-Ausecha et al., 2021). Its application involves monitoring the maturation process of climacteric fruits within the context of supply management (Ibrahim et al., 2019). Passive Radio-frequency Identification RFID tags on a conductive surface can suffer from magnetic field distortions, detuning and power loss (Ciudad et al., 2010). Magnetic field distortions due to the skin effect will cause the magnetic field lines to be almost parallel to the metal surface which leads to the inability of the antenna to harvest energy from electromagnetic induction. Detuning happens due to eddy current in the conductive surface and parasitic capacitance. Eddy current in the conductive surface produces a magnetic field that is perpendicular to the conductive surface which can lead to a reduction of total inductance (Bowler & Huang, 2005) and increases the working resonance frequency. The resonance frequency of an antenna is determined by its inductance and capacitance, following the

---

J. Zhao · C. C. Kang (✉) · J. D. Tan · M. M. Ariannejad · S. Y. C. Hoong
Department of Electrical and Electronics Engineering, Xiamen University Malaysia, Jalan Sunsuria, 43900 Sepang, Malaysia
e-mail: chiachao.kang@xmu.edu.my

J. Zhao
e-mail: eee1709521@xmu.edu.my

J. D. Tan
e-mail: jianding.tan@xmu.edu.my

M. M. Ariannejad
e-mail: mohammadmahdi.ariannejad@xmu.edu.my

S. Y. C. Hoong
e-mail: eee1904717@xmu.edu.my

S. E. Bibri et al. (eds.), *Advancing Smart Cities*, Advances in Science, Technology & Innovation,
https://doi.org/10.1007/978-3-031-52303-8_1

LC resonant frequency formula. When the inductance changes, resonance frequency also will change. Parasitic capacitance introduces parasitic impedance that causes impedance mismatch. Power loss is another issue that arises from eddy current in the conductive surface. Eddy current in the conductive surface allows the energy absorption by the conductive material which reduces the effectiveness of the antenna. Metal being conductive, possesses these three issues.

In recent years, there have been numerous researches to overcome the issues of metal surface to Ultra High Frequency (UHF) RFID tags. A loop-fed Planar Inverted—L Antenna (PILAs) was proposed for an omnidirectional UHF on-metal tag whereby four identical PILAs are placed in a rotational symmetry constellation (Lee et al., 2020). The novelty of the circular loop provides additional reactance to improve the impedance matching (Kang et al., 2017). In (Lee et al., 2019), a compact on-metal tag was designed using a pair of complementary Planar Inverted-F antennas (PIFAs) positioned in an antipodal style that reduces the size of the tag. A double T-match structure with a meander feed line antenna was applied in a design for a compact UHF RFID tag (Faudzi et al., 2014). The double T-matching technique can match the impedance of the antenna and chip easily. C-shaped antennas appear to be common in designing the antenna. In (Lee et al., 2018), a combination of a loop antenna and a PILA was applied in designing a C-shaped antenna, and the C-shaped structure is made by folding a piece of flexible substrate which contrasts with the conventional approach of using rigid printed circuit boards. Such an antenna can be easily tuned as it has multiple degrees of tuning freedom achieved by several patch segments. Another C-shaped antenna with a shorted patch was proposed by (Tan et al., 2020). The ground plane is connected to a small shorting wall and fed by a loop in the centre of a C-shaped resonator which enables flexibility in adjusting the shorting wall and the C-shaped resonator for impedance matching. A miniature folded dipole arm has achieved high compactness (Chiang et al., 2021). The dipole arms are folded into a two-fold rotational symmetrical which improves the read distance. The circular loop also provides inductance for impedance matching between the antenna and chip.

In general, there are three ways to design metal-resistant tags. The first method is to sacrifice the thickness in exchange for reducing the influence of the metal boundary of the tag by adjusting the distance between the tag antenna and the metal surface. The second method is to use absorbing material that is placed in between the antenna tag and the metal surface to reduce the effect of the metal surface. PP-4 flexible foam is used as the absorbing material (Jaakkola, 2016; Zhang & Long, 2013a, 2013b). It will absorb a portion of electromagnetic waves incident upon it. This property can help in reducing unwanted reflections and scattering from nearby surfaces, including metal. The third method is to use the substrate of the electronic band gap (EPG) structure as the dielectric plate of the antenna.

The purpose of this research is to design a compact passive UHF RFID tag that can work without magnetic distortions, detuning and power loss on a metal surface. The design required the area of the tag to be less than 50 mm by 50 mm and the thickness cannot exceed 5 mm. Besides that, the reading distance must be at least 3 m when it is placed on a metal surface with an area of 20 cm by 20 cm. The proposed antenna tag is designed in a software called CST Studio Suite, results are simulated in the software as well. CST enables users to model and evaluate electromagnetic phenomena, including antenna performance and electromagnetic fields. Through its electromagnetic simulation capabilities, CST Studio Suite enables precise modelling and analysis for the operation of tag antennas, particularly to represent the material properties of the metal surface, including its conductivity and thickness.

2 Design of the RFID Tag

2.1 Tag Chip

The tag chip that is used in the design is Monza R6 tag made by (IMPINJ, 2021). The tag chip has an equivalent circuit as shown in Fig. 1 where C_{mount} is mount capacitance, C_p is internal chip capacitance and R_p is internal resistance. Table 1 shows the parameters of Monza R6.

Based on Fig. 1, the chip impedance at different frequencies can be calculated. The total capacitance, C, is

$$C = C_p + C_{mount} \tag{1}$$

The imaginary part of the chip impedance, R_{im}, is the inductance of the chip, X_C, which can be calculated according to Eq. (2) where f is the frequency driving the tag.

$$R_{im} = X_C = -\frac{1}{2\pi f C} \tag{2}$$

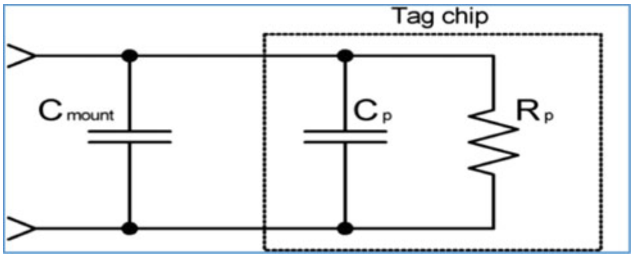

Fig. 1 Monza R6 tag chip linearized RF model (IMPINJ, 2021)

Table 1 Parameters of Monza R6 (IMPINJ, 2021)

Parameters	Typical value
C_p	1.23 pF
R_p	1.2 kΩ
C_{mount}	0.21 pF
Chip read sensitivity	−20 dBm
Chip write sensitivity	−16.7 dBm

With the information on the chip inductance, the real part of the chip impedance, R_{re}, can be calculated according to Eq. (3)

$$R_{re} = \frac{RX_C^2}{R^2 + X_C^2} \tag{3}$$

By substituting Eq. (2) into Eq. (3), Eq. (3) then becomes

$$R_{re} = \frac{R}{R^2(2\pi fC)^2 + 1} \tag{4}$$

2.2 Measuring Read Distance

The read distance is only theoretical based on mathematical calculations. Friis transmission equation is adopted for calculating the read distance. The Friis transmission equation is given as

$$\frac{P_r}{P_t} = \left(\frac{\lambda}{4\pi R}\right)^2 G_t G_r \tag{5}$$

where P_t is the radiated power of the transmitting antenna, P_r is the power received by the receiving antenna, G_t is the gain of the transmitting antenna, G_r is the gain of the receiving antenna, λ is the wavelength of the radiowave and R is the distance between the transmitting and receiving antenna. By rearranging Eq. (5), the distance R is

$$R = \frac{\lambda}{4\pi}\sqrt{\frac{P_t G_t G_r}{P_r}} \tag{6}$$

By multiplying P_r with the coefficient of power transmission of the tag, τ, it becomes the activation power of the tag chip, P_{th} (also known as reading sensitivity). Replacing P_r with P_{th} in Eq. (6), the reading distance of the tag can be calculated as in Eq. (7)

$$R = \frac{\lambda}{4\pi}\sqrt{\frac{P_t G_t G_r}{P_{th}}} \tag{7}$$

The value of τ can be calculated either from Eqs. (8) or (9) where R_C is chip resistance, R_a is antenna tag resistance, Z_C is chip impedance, Z_a is antenna tag impedance and Γ is coefficient of reflection.

$$\tau = \frac{4R_C R_a}{|Z_C + Z_a|^2} \tag{8}$$

$$\tau = 1 - \Gamma^2 \tag{9}$$

The coefficient of reflection Γ can be obtained from the S_{11} curve in CST software. Its value is equal to the value of S_{11} at the resonant frequency point after matching the impedance of the antenna tag and the chip (Ng et al., 2019).

2.3 Modelling

The proposed antenna tag in this paper adopted a combination of two methods to reduce the effect of a metal surface on the antenna tag. The two methods used are increasing the distance between the antenna tag and the metal surface and placing an absorbing material in between the antenna tag and the metal surface. In between the antenna and the metal surface, PP-4 flexible foam is used as the gap and three polyimide films are inserted which act as absorbing materials. The designed antenna has a shape similar to the pattern of 'S' which can reduce the size of the tag and the structure allows flexibility in adjusting the antenna impedance.

Figure 2 shows the 3D view of the proposed antenna tag. The structure of the entire tag can be divided into three layers, each layer is detailed in the following Sects. 2.3.1, 2.3.2 and 2.3.3. The explanation of the model takes a top-down approach that begins with the top layers, stack by stack down to the bottom layer.

2.3.1 Top Layer

The top layer of the antenna tag is an S-shaped copper sheet embedded with the Monza R6 chip as shown in Fig. 3 along with the design parameters. Such a shape allows flexibility in

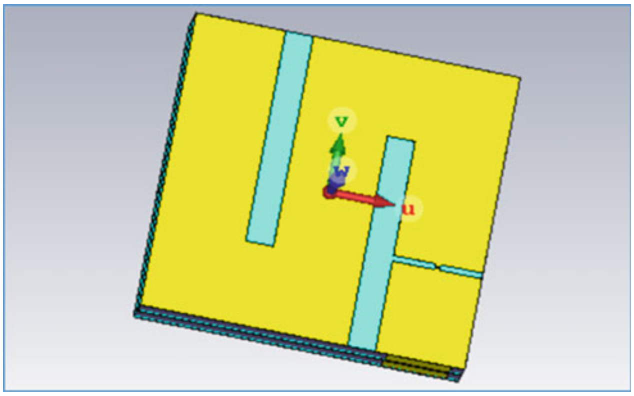

Fig. 2 3D view of the proposed antenna tag (*Source* The author)

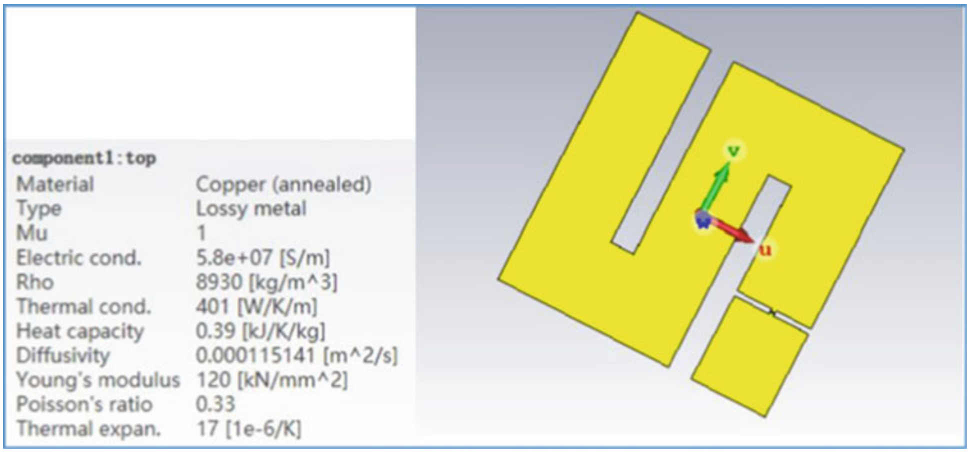

component1:top

Material	Copper (annealed)
Type	Lossy metal
Mu	1
Electric cond.	5.8e+07 [S/m]
Rho	8930 [kg/m^3]
Thermal cond.	401 [W/K/m]
Heat capacity	0.39 [kJ/K/kg]
Diffusivity	0.000115141 [m^2/s]
Young's modulus	120 [kN/mm^2]
Poisson's ratio	0.33
Thermal expan.	17 [1e-6/K]

Fig. 3 Top layer of the tag and design parameters (*Source* The author)

adjusting parameters and helps in reducing the size of the tag. The thickness of this layer is 0.009 mm.

2.3.2 Middle Layer

On the top of the middle layer are polyimide film (film 1) and flexible foam (foam 1) as shown in Figs. 4 and 5 along with the design parameters respectively. Film 1 absorbs electromagnetic waves generated by electromagnetic induction on the metal surface whereas foam 1 increases the gap between the antenna and the metal surface and provides structural bending capability. The thicknesses of film 1 and foam 1 are 0.05 mm and 1.6 mm respectively.

The centre part of the middle layer is a small U-shaped arm copper sheet (U-arm) connected to the top layer by a copper patch (Cu-patch) as shown in Figs. 6 and 7 along with the design parameters. The function of the U-arm is to increase the electrical length of the antenna to adjust the impedance of the antenna.

On the bottom of the middle layer are two identical polyimide films (film 2; film 3) stacked on the top of a flexible foam (foam 2) as shown in Figs. 8 and 9 along with the design parameters respectively. Film 2 and film 3 are identical to film 1 and share the same function as film 1. The use of foam 2 has the same function as foam 1 and it's identical to foam 1.

2.3.3 Bottom Layer

The bottom layer is made of a copper sheet (Cu-btm) connected to the top layer and U-arm by two small copper patches as shown in Figs. 10 and 11 along with the design parameters. Cu-btm has the same function as U-arm which is to adjust the impedance of the antenna. This layer has a thickness of 1.6 mm.

2.4 Tag Dimension

Figure 12a shows the 2-dimensional view of the tag's top layer and sides where "Shorting Wall A" and "Shorting Wall B" correspond to the copper patches. Figure 12b shows the 2-dimension of the middle layer of the tag. Table 2 shows all the dimensional values in Fig. 12.

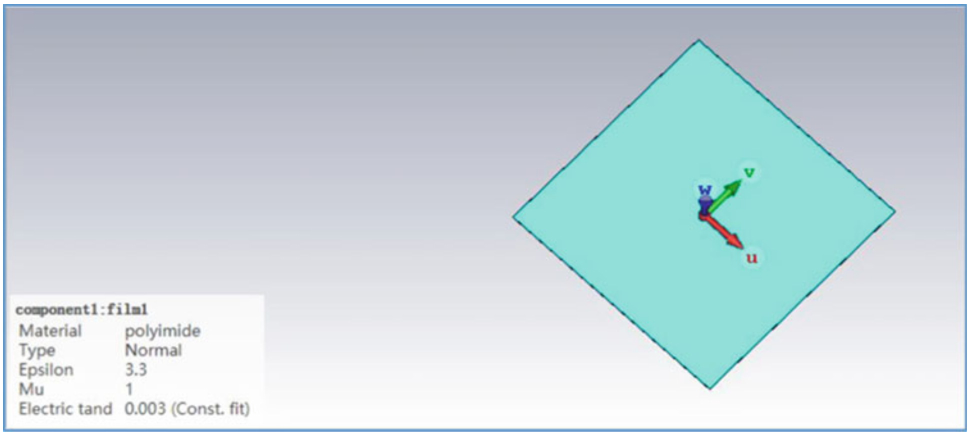

component1:film1

Material	polyimide
Type	Normal
Epsilon	3.3
Mu	1
Electric tand	0.003 (Const. fit)

Fig. 4 Polyimide film and design parameters (film 1) (*Source* The author)

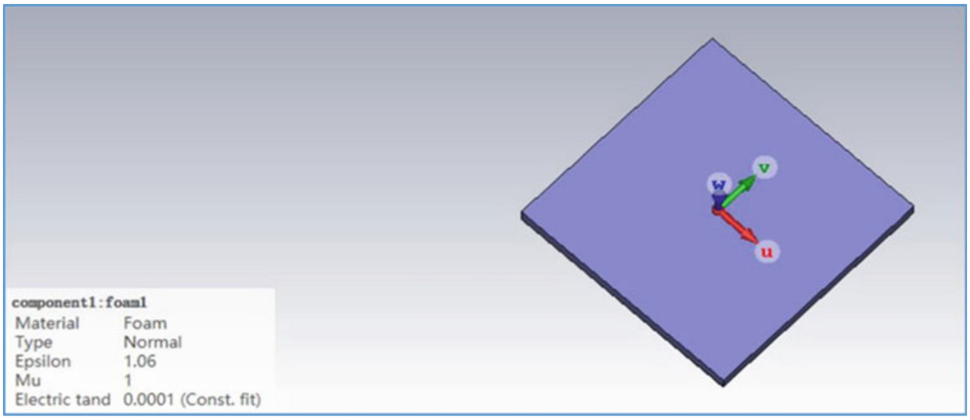

component1:foam1

Material	Foam
Type	Normal
Epsilon	1.06
Mu	1
Electric tand	0.0001 (Const. fit)

Fig. 5 Flexible foam and design parameters (foam 1) (*Source* The author)

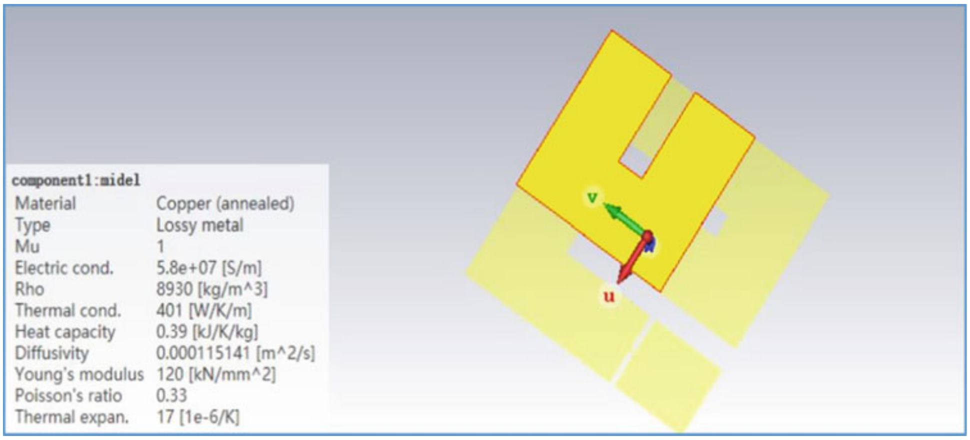

component1:midel

Material	Copper (annealed)
Type	Lossy metal
Mu	1
Electric cond.	5.8e+07 [S/m]
Rho	8930 [kg/m^3]
Thermal cond.	401 [W/K/m]
Heat capacity	0.39 [kJ/K/kg]
Diffusivity	0.000115141 [m^2/s]
Young's modulus	120 [kN/mm^2]
Poisson's ratio	0.33
Thermal expan.	17 [1e-6/K]

Fig. 6 U-shaped arm and design parameters (U-arm) (*Source* The author)

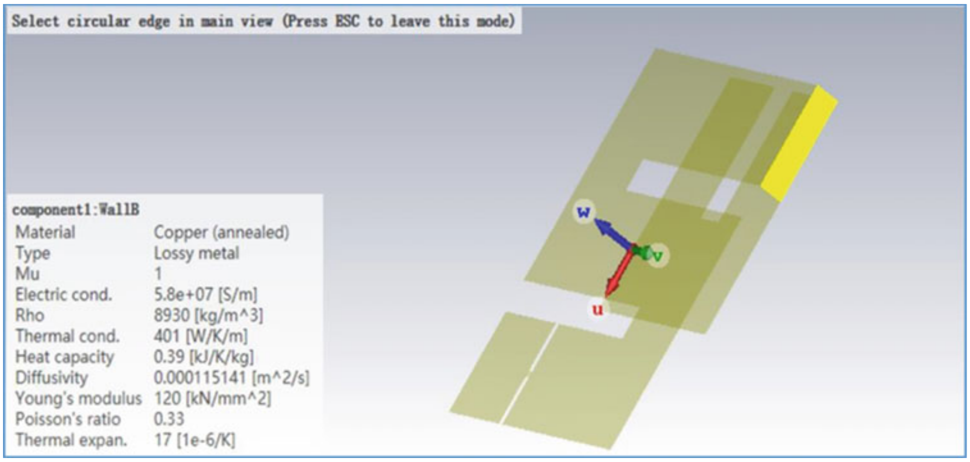

Select circular edge in main view (Press ESC to leave this mode)

component1:WallB

Material	Copper (annealed)
Type	Lossy metal
Mu	1
Electric cond.	5.8e+07 [S/m]
Rho	8930 [kg/m^3]
Thermal cond.	401 [W/K/m]
Heat capacity	0.39 [kJ/K/kg]
Diffusivity	0.000115141 [m^2/s]
Young's modulus	120 [kN/mm^2]
Poisson's ratio	0.33
Thermal expan.	17 [1e-6/K]

Fig. 7 Copper patch and design parameters (Cu-patch) (*Source* The author)

2.5 Impedance Matching

The one last factor that must be decided for the impedance matching of the antenna tag and antenna chip is the frequency band of the antenna. This can be done in the CST software by sweeping the frequency of the antenna and plotting its impedance. Table 3 shows the Monza R6 chip impedance at different frequencies.

With the matching frequency, the bandwidth can be determined by plotting the S_{11} (note that S_{11} is equal to the coefficient of reflection, Γ) parameters against frequency. Figure 13 shows the plot where the lowest point at 930.98 MHz has a S_{11} value of −10.6141 dB. The bandwidth selected has a range of 927.45–935.1 MHz where the S_{11} values are lower than −3 dB.

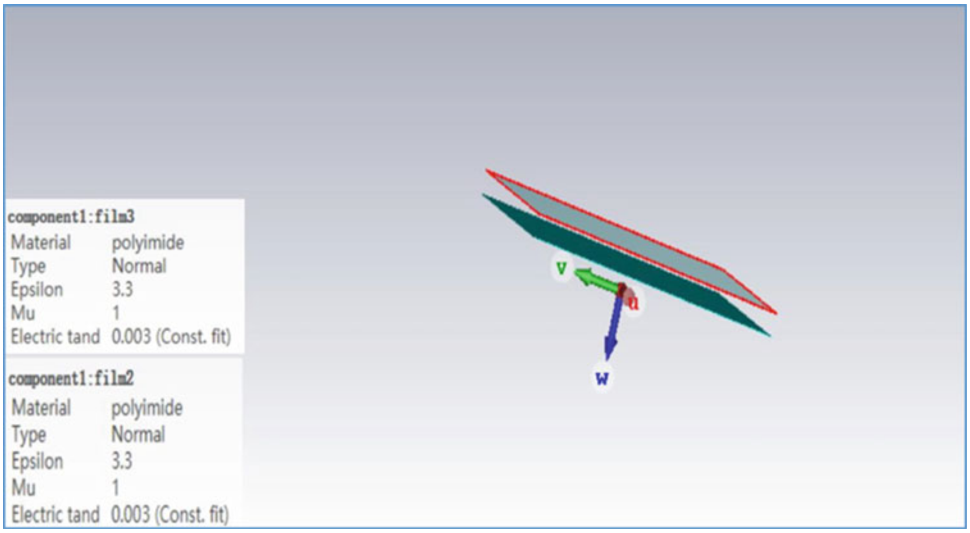

Fig. 8 Identical polyimide films and design parameters (film 2; film 3). (*Source* The author)

component1:film3

Material	polyimide
Type	Normal
Epsilon	3.3
Mu	1
Electric tand	0.003 (Const. fit)

component1:film2

Material	polyimide
Type	Normal
Epsilon	3.3
Mu	1
Electric tand	0.003 (Const. fit)

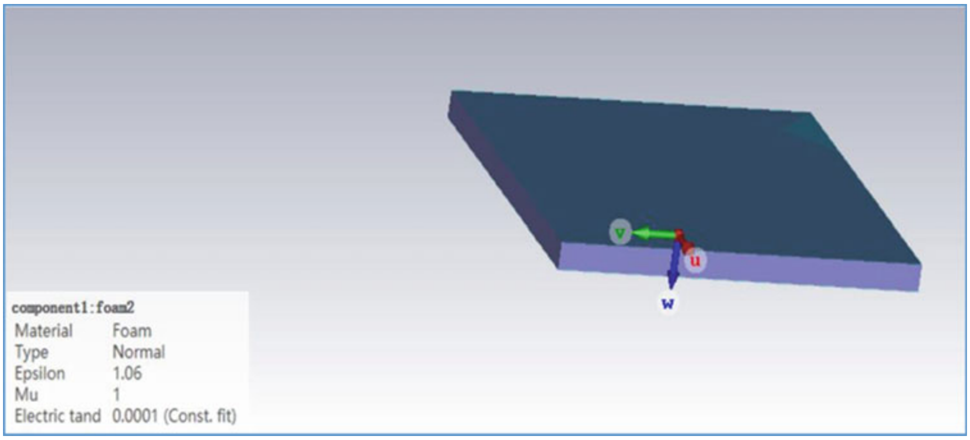

Fig. 9 Flexible foam and design parameter (foam 2) (*Source* The author)

component1:foam2

Material	Foam
Type	Normal
Epsilon	1.06
Mu	1
Electric tand	0.0001 (Const. fit)

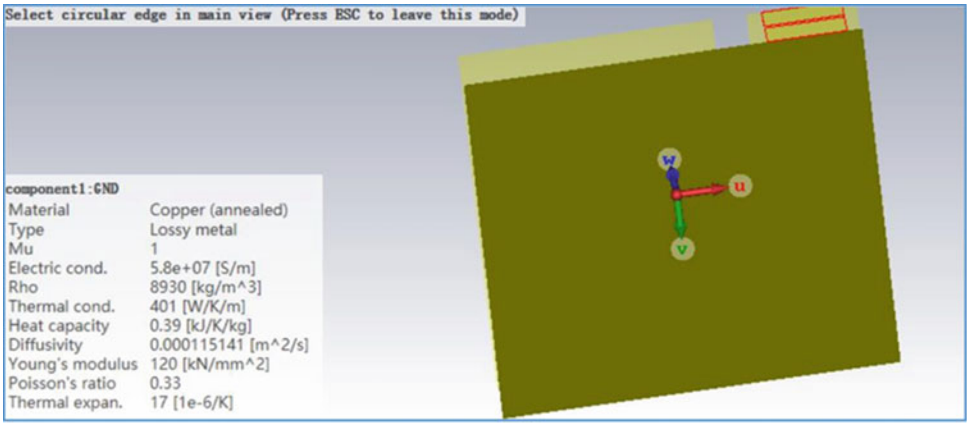

Fig. 10 Bottom of the tag—bottom copper plate (Cu-btm) (*Source* The author)

Select circular edge in main view (Press ESC to leave this mode)

component1:GND

Material	Copper (annealed)
Type	Lossy metal
Mu	1
Electric cond.	5.8e+07 [S/m]
Rho	8930 [kg/m^3]
Thermal cond.	401 [W/K/m]
Heat capacity	0.39 [kJ/K/kg]
Diffusivity	0.000115141 [m^2/s]
Young's modulus	120 [kN/mm^2]
Poisson's ratio	0.33
Thermal expan.	17 [1e-6/K]

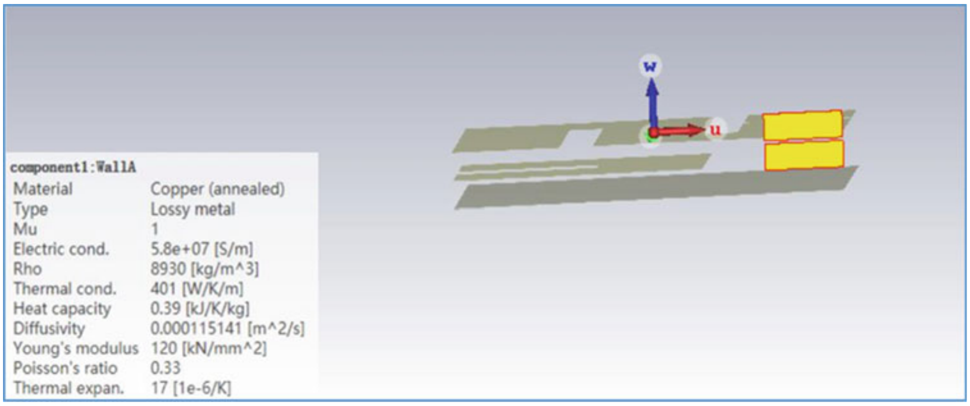

component1:WallA

Material	Copper (annealed)
Type	Lossy metal
Mu	1
Electric cond.	5.8e+07 [S/m]
Rho	8930 [kg/m^3]
Thermal cond.	401 [W/K/m]
Heat capacity	0.39 [kJ/K/kg]
Diffusivity	0.000115141 [m^2/s]
Young's modulus	120 [kN/mm^2]
Poisson's ratio	0.33
Thermal expan.	17 [1e-6/K]

Fig. 11 Identical coper patches and design parameters (Cu-ground-patch) (*Source* The author)

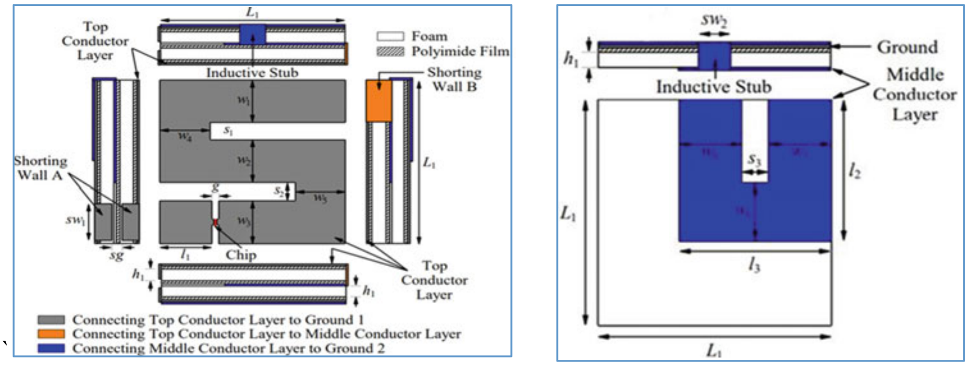

(a) (b)

Fig. 12 2-dimensional view of the tag **a** top layer and sides **b** middle layer (Ng et al., 2019)

Table 2 Dimensional values of the tag (Ng et al., 2019)

Symbol	Value (mm)
L_1 (*Width*)	25
h_1 (*Thickness*)	1.6
$w_1, w_2, w_3, w_7 w_8$	6.9
w_4, w_5, w_6	7
s_1, s_2	2.15
s_3	2.7
g	0.5
sg	0.2
sw_1	5
sw_2	2.9
l_1	7.75
l_2	16
l_3	16.75
t	0.009

Table 3 Monza R6 chip impedance at different frequencies (IMPINJ, 2021)

Frequency (MHz)	Impedance (Ω)
860	13.608–j128.517
916	12.011–j120.660
920	11.908–j120.135
921	11.882–j120.004
922	11.857–j119.874
923	11.831–j119.744
924	11.806–j119.615
925	11.781–j119.486
926	11.755–j119.357
927	11.730–j119.228
928	11.705–j119.099
929	11.680–j118.871
930	11.655–j118.843
931	11.631–j118.716
932	11.606–j118.588
933	11.581–j118.461
934	11.557–j118.334
935	11.532–j118.208

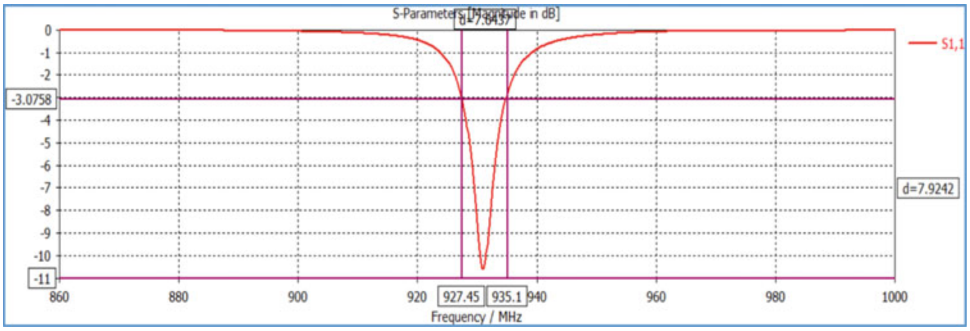

Fig. 13 S_{11} parameters against frequency and bandwidth selection (*Source* The author)

3 Simulation Results

3.1 Electromagnetic Fields

Electric field intensity observed around the top layer of the tag is averaging at 20000 V/m as shown in Fig. 14. The maximum electric field strength at a point is 161613 V/m. The magnetic field distribution around the top layer of the tag is as shown in Fig. 15. This field distribution provides insights into how the magnetic field strength varies in the vicinity of the tag's upper layer. The magnetic field is peaked at 152.68 A/m at a point. This indicates the maximum strength of the magnetic field at that specific point.

3.2 Theoretical Read Distance and Coefficient of Power Transmission

The antenna tag read distance is based on the Friss transmission equation, Eq. (5). The equation provides and determines the travel distance of the tag signal before the signal becomes too weak to be detected. P_{th} is assumed to be the chip reading sensitivity which is −20 dBm or 0.01 mW. This value acts as a threshold for assessing whether the received signal is strong enough for the chip to correctly interpret it. Transmitting antenna is assumed to operate with 4 W EIRP which is equal to the product of P_t and G_t. Table 4 shows the read distance, R, of two different values G_r.

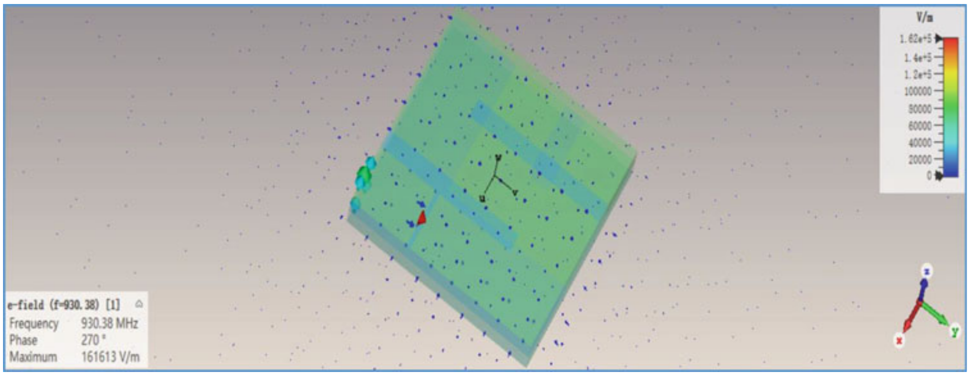

Fig. 14 Electric field around the top layer of the tag (*Source* The author)

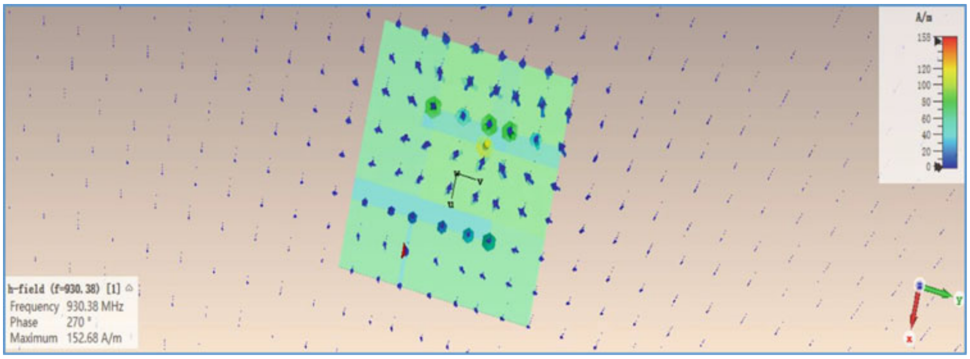

Fig. 15 Magnetic field around the top layer of the tag (*Source* The author)

Table 4 Tag read distance (*Source* The author)

G_r(dBi)	R (m)
−11.4	4.271
−10.36	4.815

4 Conclusion

A compact S-shaped metal mountable UHF RFID tag is designed in software named CST Studio Suite. Monza R6 chip has been selected as the tag chip. Two methods are used to model the tag which is increasing the gap between the antenna and the metal surface, and placing absorbing material between the antenna and the metal surface. PP-4 flexible foam is used as the gap and three polyimide films are inserted which act as absorbing materials. The antenna is S-shaped which helps in tag size reduction and provides flexibility over impedance matching. The resulting dimension of the tag is 25 mm by 25 mm by 3.377 mm which is small in size. The impedance matching frequency is 930.98 MHz where the impedance of the antenna is 6.350 + j119.157 Ω and the impedance of the chip is 11.631–j118.716 Ω. The coefficient of power transmission of the tag is 0.913. Thus, the tag is able to achieve a reading distance of up to 4.815 m given that G_r is −10.36 dBi. Due to the prevalence of metal objects in supply chains, on-metal RFID tag antennas are essential for the precise tracking of supplies. Without being hampered by the presence of metal, these antennas allow for the seamless integration of RFID technology into supply chain procedures and other potential applications. Conducting this research will expand our knowledge related to the challenges posed by metal interferences and lead to more reliable identification and tracking of tagged items. The finding from the study could be policy implications related to industries such as healthcare, manufacturing or aviation.

Acknowledgements The author gratefully acknowledges financial support from the Malaysian Ministry of Higher Education under Fundamental Research Grant Scheme: FRGS/1/2022/TK08/XMU/02/10 and Xiamen University Malaysia under Research Fund Grant No: XMUMRF/2021-C7/IECE/0018 and XMUMRF/2023-C12/IECE/0047.

References

Bowler, N., & Huang, Y. (2005). Electrical conductivity measurement of metal plates using broadband eddy-current and four-point methods. *Measurement Scientific and Technology, 16*(11), 2193–2200. https://doi.org/10.1088/0957-0233/16/11/009.

Chiang, S. M., Lee, T. L., Lim, E. H., Chee, P. S., Lee, Y. H., Bong, F. L., Phua, Y. N., & Chung, B. K. (2021). Miniature folded dipole in rotational symmetry for metal tag design. *Progress in Electromagnetics Research C, 110*, 55–66. https://doi.org/10.2528/PIERC2012062.

Ciudad, D., Cobos, P., Sanchez, P., & Aroca, C. (2010). RFID in Metal Environments: An overview on low (LF) and ultra-low (ULF) frequency system led. *Research Gate.* https://doi.org/10.5772/7978.

Fahmy, A., Altaf, H., Al Nabulsi, A., Al-Ali, A., & Aburukba, R. (2019). Role of RFID technology in smart city applications. In *IEEE International Conference on Communications, Signal Processing, and Their Applications* (*ICCSPA*) (pp. 1–6). https://doi.org/10.1109/ICCSPA.2019.8713622.

Faudzi, N. M., Ali, M. T., Ismail, I., Jumaat, H., & Sukaimi, N. H. (2014). Metal mountable UHF-RFID tag antenna with meander feed line and double T-match. In *IEEE 2014 International Symposium on Technology Management and Emerging Technologies* (*ISTMET*) (pp. 33–38). https://doi.org/10.1109/istmet.2014.6936473.

Ibrahim, A. A. A., Nisar, K., Hzou, Y. K., & Welch, I. (2019). Review and analyzing RFID technology tags and applications. In *IEEE 13th International Conference on Application of Information and Communication Technologies* (*AICT*) (pp. 1–4). https://doi.org/10.1109/AICT47866.2019.8981779.

IMPINJ. (2021). *Monza R6 Tag Chip Datasheet IPJ-W1700-K00 Version 7*. https://support.impinj.com/hc/en-us/articles/202765328-Monza-R6-ProductBrief-Datasheet.

Jaakkola, K. (2016). Small on-metal UHF RFID transponder with long read range. *IEEE Transactions on Antenna and Propagation, 64* (11), 4859–4867. https://doi.org/10.1109/TAP.2016.2607752.

Kang, C. C., Teh, Y. H., Tan, J. D., Mohammad, M. A., & Siti, B. (2023). Review of 5G wireless cellular network on Covid-19 pandemic: Digital healthcare & challenges. *Jurnal Kejuruteraan, 35* (3), 02.

Kang, C. C., Ain, M. F., Zalzala, A. M., & Zubir, I. A. (2017). Lumped element equivalent circuit modelling for RF energy harvesting antenna array. In *9th International Conference on Robotic, Vision, Signal Processing and Power Applications* (pp. 455–461). Springer. https://doi.org/10.1007/978-981-10-1721-6_49.

Lee, Y. H., Lim, E. H., Bong, F. L., & Chung, B. K. (2020). Loop-Fed Planar Inverted-L Antennas (PILAs) for omnidirectional UHF on-metal tag design. *IEEE Transactions on Antennas and Propagation, 68*(8), 5864–5871. https://doi.org/10.1109/TAP.2020.2990287.

Lee, Y. H., Lim, E. H., Bong, F. L., & Chung, B. K. (2018). Compactfolded C-shaped antenna for metal- mountable UHF RFID applications. In *IEEE Transactions on Antennas and Propagation.* https://doi.org/10.1109/TAP.2018.2879853.

Lee, Y. H., Lim, E. H., Bong, F. L., Chung, B. K., & Lee, K. Y. (2019). Complementary planar Inverted- F antenna (PIFAs) for On-Metal RFID Tag Design. In *2019 IEEE Asia-Pacific Conference on Applied Electromagnetic* (*APACE*). https://doi.org/10.1109/APACE47377.2019.9020868.

Munoz-Ausecha, C., Ruiz-Rosero, J., & Ramirez-Gonzalez, G. (2021). RFID applications and security review. *Computation, 9*(6), 69. https://doi.org/10.3390/computation9060069.

Ng, W. H., Lim, E. H., Bong, F. L., & Chung, B. K. (2019). Compact planar inverted- S antenna with embedded tuning arm for on-metal UHF RFID tag design. *IEEE Transactions on Antennas and Propagation, 67*(6), 4247–4252. https://doi.org/10.1109/TAP.2019.2911191.

Tan, N. M., Lin, Y. F., Chang, C. H., Liao, C. T., & Chen, H. M. (2020). Compact shorted C-shaped patch antenna for UHF RFID tag mounted on metallic objects. In *2020 International Workshop on Electromagnetics: Applications and Student Innovation Competition* (*iWEM*). https://doi.org/10.1109/iWEM49354.2020.9237434.

Zhang, J., & Long, Y. (2013a). A dual-layer broadband compact UHF RFID tag antenna for platform tolerant application. *IEEE Transactions on Antennas and Propagation, 61*(9), 4447–4455. https://doi.org/10.1109/TAP.2013.2269472.

Zhang, J., & Long, Y. (2013b). A miniaturized via-patch loaded dual-layer RFID tag antenna for metallic object applications. *IEEE Antennas and Wireless Propagation Letters, 12*, 1184–1187. https://doi.org/10.1109/LAWP.2013.2281842.

Assessment of Speech Intelligibility in Buildings with Low Reverberation

Sara Girón, Javier Alayón, Teresa Gómez-Gómez,
and Francisco J. Nieves

Abstract

This work is based on the results of listening tests designed through the comparison of two signals in order to investigate the subjective perception of speech intelligibility in public venues with low reverberation. Binaural impulse responses obtained in a campaign of acoustic measurements in a set of Roman theatres in Spain, built in the imperial era in what was then the province of Hispania, have been convolved with anechoic recordings of oral texts with male and female voices to produce the signals of comparison of the tests across the whole range of values of the acoustic parameter Speech Transmission Index (STI). This is a single-value parameter that integrates the significant spectral data of speech. These performance venues were built in classical times of Western civilisation for theatrical performances and other oral events where speech intelligibility played a primary role. They present short reverberation times at medium frequencies, between 0.33 s and 2.32 s, depending on the size and state of rehabilitation of the space. The tests were completed in a semi-anechoic acoustic laboratory in the School of Architecture of the University of Seville, and the design of the comparison pairs therein is based on the method of limits used in neuroscience. The statistical analysis of the results by means of Pearson's non-parametric chi-square test carried out by the SPSS software has been undertaken to study the correlations of the responses obtained; these correlations depend on whether it is the ascending or descending series of stimuli, and on the voice format, the gender, and sociological data of the respondents. Furthermore, an estimation is carried out of the differential limen of the STI parameter. The findings of this study are useful in the smart city context and urban planning, especially in public open-air venues.

Keywords

Listening test • Smart venues • Roman theatres • Speech intelligibility • Method of limits • Differential limen

1 Introduction and Research Objectives

Speech is vital in human communication although the speech signal can sometimes be degraded by the transmission path between the talker and the listener, thereby resulting in a reduction in the intelligibility of the speech at the listener point. The speech transmission index (STI) method quantifies the deterioration of the speech signal induced by a transmission channel. The objective STI has been refined since its introduction in the 1970s by Houtgast & Steeneken, and major improvements have been consolidated through their incorporation in successive revisions of the International Electrotechnical Commission, IEC-60268-16 standard. Since 1988, this standard has been revised several times, with the latest revision (Edition 5) appearing in 2020. Research carried out by the scientific community on the STI parameter has led to the incorporation of improvements into successive editions of the standard. These include redundancy factors for neighbouring bands, level-dependent auditory masking, various procedures to apply the STI parameter to special groups of people, such as non-natives and the hearing-impaired, and enhancements to

---

S. Girón (✉) · J. Alayón · F. J. Nieves
Departamento de Física Aplicada II e Instituto Universitario de Arquitectura y Ciencias de la Construcción, Universidad de Sevilla, Av. Reina Mercedes 2, 41012 Seville, Spain
e-mail: sgiron@us.es

J. Alayón
e-mail: jap01@us.es

F. J. Nieves
e-mail: nieves@us.es

T. Gómez-Gómez
Departamento de Estadística e Investigación Operativa, Facultad de Matemáticas, Universidad de Sevilla, Calle Tarfia, 41012 Seville, Spain
e-mail: terego@us.es

S. E. Bibri et al. (eds.), *Advancing Smart Cities*, Advances in Science, Technology & Innovation,
https://doi.org/10.1007/978-3-031-52303-8_2

STI data to improve the effects of environmental noise and speech levels in simulations.

The just noticeable difference (JND) or differential limen is the minimal variation in the value of an acoustic parameter that is detectable by a listener. This descriptor is accepted as a great indicator of the subjective perception caused by the variation of a parameter and is very useful in a large number of applications in room acoustics: it offers guidance on the precision with which the objective acoustic parameters should be measured; it establishes the accuracy with which computational models should be able to simulate an enclosure; and it constitutes a fundamental tool for acousticians to ascertain whether an alteration in the design of a room would indeed be appreciated by the audience.

In this regard, Cremer & Muller (1982), described the results of the JND for reverberation time *T* and pointed out that for longer times than 0.6 s the JND was approximately 4% relative to the measured value, while for shorter than 0.6 s the differential limen became absolute and approximately equal to 0.024 s.

By using synthetic sound fields, Reichardt & Schmidt (1967) studied the detectability of level changes, the delay of reflections, and the reverberation onset in an impulse response. Measured results were expressed in terms of differential thresholds, and they also studied the variations in the sound field necessary for detection by 50% of listeners.

Regarding energy parameters based on impulse responses and related to speech intelligibility, Cox et al. (1993) provided a detailed discussion on JND of several acoustic descriptors also based on synthetic sound fields similar to those encountered in concert halls. Additional research was carried out by Bradley et al. (1999) that focused on clarity of speech C_{50}. It considered three reverberation times, varying from 0.5 s to 2.0 s, and concluded that, under the observed conditions, the JND for C_{50} was 1.1 dB and was independent of reverberation time. The authors proposed that the corresponding JND for STI be 0.03 by correlation with the differential limen of other energy parameters indicating speech intelligibility, but no direct studies of the JND for this parameter have yet been published.

With actual acoustic fields, Martellotta (2010) studies the differential limen of centre time and clarity parameters in large reverberant places such as churches, while Liu et al. (2020), through listening tests of intelligibility in Mandarin Chinese, explore the factors that influence the intelligibility of speech in large venues. From their results, they propose another scale of valuation of STI for large spaces.

This work is based on the results of listening tests designed through the comparison of two signals in order to investigate the subjective perception of speech intelligibility in public venues with low reverberation. The intelligibility study has been carried out through the STI parameter and its differential limen. These results are of interest for the assessment of acoustic comfort and speech intelligibility in outdoor venues within the scope of smart cities and urban design (Yang & Kang, 2005).

1.1 The STI Parameter

The single-index STI is a monaural parameter that assumes values between 0 (zero intelligibility) and 1 (optimal intelligibility). Its calculation is complex and is based on the modulation transfer function (MTF). To this end, it involves 7 carrier octave bands *i* corresponding to the human voice (125 Hz–8000 Hz) with 14 modulation frequencies *k* (one-third octave interval range from 0.63 Hz up to 12.5 Hz), thereby obtaining the modulation matrix of 98 values.

The modulation reduction factor *m* of a room can be deduced from the impulse response (Schroeder, 1981) called the indirect method. Cabrera et al. (2014) also discuss the causes of vulnerability in several commercial tools of the indirect method of measuring STI and provide a robust freely available implementation, executed by the authors.

In this method, to appraise the modulation reduction factor in octave band *i*, and modulation frequency F_K $m_i(F_k)$, first the impulse response *h(t)* must be filtered in the seven frequency bands *i* [$h_i(t)$] (Zamarreño et al., 2008; International Electrotechnical Commission, IEC 60268–16 2020). Hence $m_i(F_k)$ can be obtained as the Fourier transform of the squared impulse response as:

$$m_i(F_k) = \frac{\int_0^\infty h_i^2(t)\, e^{-j2\pi F_k t} dt}{\int_0^\infty h_i^2(t)\, dt}. \tag{1}$$

These modulation reduction factor $m_i\ (F_k)$ values are converted to effective signal-to-noise ratios SNR_{eff} by the expression:

$$SNR_{\mathrm{eff}ik} = 10 \log\left(\frac{m_i(F_k)}{1 - m_i(F_k)}\right)(\mathrm{dB}). \tag{2}$$

These 98 values are limited to the −15 dB + 5 dB range so that the STI remains within the 0–1 margin. In a room, the main distortions involved in the loss of modulation are reverberation and background noise. When both factors affect the signal, the total modulation reduction factor can be obtained as the product of these two factors:

$$m = m_{rev} \cdot m_{noise} = \frac{1}{\sqrt{1 + \left(\frac{2\pi F_k T_i}{13.82}\right)^2}} \cdot \frac{1}{1 + 10^{\frac{-SNR_{ik}}{10}}}. \tag{3}$$

In this equation, T_i is the early decay time at each octave band (alternatively, the reverberation time) under diffuse field hypothesis, and F_K is the modulation frequency.

From the modulation reduction matrix, the averaged values for the 14 modulation frequencies enable the

Table 1 Standard scale of valuation of the STI parameter versus speech intelligibility (Acoustics Engineering 2002)

STI	0.00–0.30	0.30–0.45	0.45–0.60	0.60–0.75	0.75–1.00
Speech intelligibility	Bad	Poor	Fair	Good	Excellent

modulation indices (MTI) to be calculated and then the STI parameter can be calculated as the weighted sum of MTI for each octave band.

The qualification of intelligibility for a native listener with normal hearing in terms of the STI parameter, validated with subject-based intelligibility experiments, is shown in Table 1 and is independent of language.

2 Methods

This section describes the experimental system employed to obtain the impulse responses and hence the STI indices in the Roman theatres studied. The most important characteristics of the seven Roman theatres are briefly described, the anechoic material used for the auralisation of the signals that intervene in the surveys is presented, and finally, the listening test and the procedure for carrying out the surveys are explained.

2.1 Experimental Set-Up

In the Roman theatres, the acoustic experimental measurements were carried out without the public by following the protocol established in the International Organisation for Standardisation, ISO 3382 part 1 (2009), and part 2 (2008), which affect the recommended source–receiver number of combinations and the monitoring of environmental conditions (temperature, relative humidity, and air velocity), among other recommendations.

The theatres were acoustically excited to obtain the room impulse responses (RIRs) at the reception points by means of sine-swept signals of variable duration of up to 20 s depending on the theatre, wherein the frequency grows exponentially over time from 20 Hz to 20,000 Hz. These signals have been produced and processed by commercial software platforms (EASERA v1.2 and IRIS) connected to the rest of the measurement chain through AUBIONx8 and MOTU 4PRE HYBRID sound cards, respectively. The omni-directional source used was an AVM DO-12 located 1.50 m above the floor (in the centre and lateral part of the scaena, and in the centre of the orchestra), and previous amplification with a B&K 2734-type power amplifier, the excitation signals were reproduced in the spaces. The RIRs were captured either by means of the omni-directional and figure-of-eight configurations of an Audio-Technica AT4050/CM5 microphone connected to a Sound Field SMP200 polarisation source or via the Core Sound TetraMic microphone array. A Head Acoustics HMS III torso simulator (Code 1323) and a B&K 2829 microphone polarisation source were employed to capture the binaural RIRs. In all cases, microphones were located 1.20 m from the floor at a variable number of reception points ranging from 18 in Regina Turdulorum theatre to 35 in Saguntum theatre. The processing of the impulse responses enabled the monaural and binaural acoustic parameters as well as the STI at the positions of the microphones to be known. A Svantek SVAN 958 analyser recorded the background noise level. More details regarding the experimental chain can be found in Girón et al. (2021).

2.2 The Roman Theatres

Hispania is the Roman name attributed to the Roman provinces located on the Iberian Peninsula and the Balearic Islands. The period of Rome's domination in this territory starts with the landing in Ampurias in 218 BC and lasted until the beginning of the fifth century with the entry of the Visigoths into the peninsula: during the Visigoth period this name was also maintained. These classical precincts of Western civilisation were built for theatrical performances and other oral events where intelligibility played a primary role. Of the Roman theatres documented and located in Hispania, 22 remain in present-day Spain, and 3 in present-day Portugal (Braga, Lisbon, and Evora). Of those in Portugal, only traces of the theatres remain.

Hispania was converted into a fundamental part of the Roman Empire, as evidenced by the large number of monuments for public assembly and performance in the region (Girón et al., 2021).

The PIAATRE research project, developed at the University of Seville, considers the study of the intangible cultural heritage of the sound of Roman theatres to be a key factor in European identity, not only in the current identity but also in the past (acoustic archaeology) and the future (restoration projects, intervention, and ephemeral architecture). In this project, the following 7 theatres, located in three ancient Roman provinces (Fig. 1), have been acoustically measured in situ, in alphabetical order:

Carthago Nova (Cartagena, Murcia), Fig. 2; Emerita Augusta (Merida, Badajoz), Fig. 3; Italica (Santiponce, Seville), Fig. 4; Metellinum (Medellin, Badajoz), Fig. 5;

Fig. 1 The five provinces of Hispania established by Emperor Diocletian with their capitals marked in red. (*Source* the authors)

Fig. 2 View of the Carthago Nova theatre (*Source* Romero-Odero, J. A.; PIAATRE project)